



Cresswell, A.J. , Sanderson, D.C.W. , Carling, P.A. and Darby, S.E. (2022)
Quartz age extension applied to SE Asian cover sands. *Quaternary
Geochronology*, 69, 101271. (doi: [10.1016/j.quageo.2022.101271](https://doi.org/10.1016/j.quageo.2022.101271))

The material cannot be used for any other purpose without further
permission of the publisher and is for private use only.

There may be differences between this version and the published version.
You are advised to consult the publisher's version if you wish to cite from
it.

<https://eprints.gla.ac.uk/267456/>

Deposited on 21 March 2022

Enlighten – Research publications by members of the University of
Glasgow

<http://eprints.gla.ac.uk>

1 Quartz Age Extension Applied to SE Asian Cover Sands

2
3 Cresswell, A.J.^{*1}, Sanderson, D.C.W.¹, Carling, P.A.^{2,3}, Darby, S.E.²

4
5 ¹ Scottish Universities Environmental Research Centre, Rankine Avenue, East Kilbride,
6 United Kingdom

7 ² Geography & Environmental Science, University of Southampton, UK

8 ³ Chengdu University of Technology, Chengdu, Sichuan 610059, China.

9 *Corresponding Author: alan.cresswell@glasgow.ac.uk

10 11 **Abstract**

12
13 A significant feature of the surface sediments of southeast Asia is a regionally extensive layer
14 of distinctive red, quartz-rich, cover sand observed throughout Vietnam, Cambodia, Laos and
15 Thailand, and further afield. In many locations, these cover sands immediately overlay a laterite
16 layer containing tektites, known as the Muong Nong type, associated with a large meteorite
17 impact between 750 to 800ka in Indochina. Sections of these cover sands at sites in Thailand,
18 Laos and Vietnam have been investigated using field and laboratory profiling, and quartz SAR
19 procedures. In some locations the sections consist of a layer of low-sensitivity quartz with
20 saturated signals overlain by a visibly indistinguishable layer of high-sensitivity quartz with
21 ages less than c. 35ka. Further work has been undertaken to attempt to extend quartz
22 luminescence dating for the older materials, including samples associated with the tektites,
23 using thermally stimulated or transferred luminescence to access traps that are expected to
24 saturate at higher doses. Luminescence was recorded during sample heating and hold, giving
25 thermoluminescence (TL-ramp) and isothermal decay (ID) data, in addition to optically

26 stimulated luminescence after the transfer (Thermally Transferred Optically Stimulated
27 Luminescence, TT-OSL) measurements. These measurements have produced equivalent dose
28 values of up to 250Gy, and ages of 70-125ka, for these older materials, which is significantly
29 younger than would be expected from the association with the tektites. Investigation of the
30 traps associated with these signals has produced properties consistent with prior investigations,
31 suggesting that these are not sufficiently stable at environmental temperatures above 25°C to
32 permit age extension using these methods.

33

34

35

36 **Keywords** Thermally Transferred Optically Stimulated Luminescence; Thermoluminescence;
37 Isothermal Decay

38

39 **Highlights**

40

- 41 • TT-OSL applied to coarse quartz grains from SE Asia
- 42 • Ages obtained significantly less than assumed age of associated tektites
- 43 • Thermal stability of TT-OSL traps assessed
- 44 • Thermal stability limits age range to less than 800ka at temperatures above 25°C

45 1. Introduction

46 A feature present across large parts of south east Asia (including southern China, Laos,
47 Vietnam, northern Cambodia and north east Thailand) is a distinct layer of sand. These cover
48 sands are generally red-coloured, consisting of virtually mono-mineralic quartz sand and in
49 undisturbed locations can be between 3 and 15m thick. These deposits often lie directly upon
50 the weathered, brecciated or lithified basement rocks or above a distinct gravel layer. The
51 origin of these sands is unclear, having been variously attributed to lacustrine, marine,
52 colluvial, fluvial, aeolian or biomantle processes. The literature supporting these different
53 models is summarised in Sanderson et.al. (2001), where data obtained from Khon Kaen in
54 NE Thailand with broadly concordant TL and OSL ages in the last 50 ka was interpreted as
55 supporting aeolian origins for the cover sands. Recent investigation near Huai Om in
56 Thailand identifies air-fall deposits lying above base-surge deposits in the cover sands as the
57 result of a significant regional Quaternary meteorite impact (Tada et al., 2020).

58

59 The cover sands are associated with another regional feature; an extensive area of tektite
60 deposition associated with the impact event centred over SE Asia 750-800ka BP (see, for
61 example, Schwarz et al., 2016; Jourdan et al., 2019; Michel et al. 2021). The tektite field
62 covers an area of southern Asia and Australasia of approximately 8000 x 13000 km, from
63 Madagascar into the Pacific Ocean, southern China to all of Australia and potentially into
64 Antarctica (see, for example, Whymark, 2021). In SE Asia, lateritic granule layers within the
65 lower section of the cover sands contain tektites from this impact, with many of them
66 appearing to be undisturbed since deposition (Tada et al, 2020). The details of the
67 stratigraphic relationships of the cover sands with the underlying gravels and tektites will be
68 presented in a future paper, but are summarized within Figure 1. In the work presented here,
69 the optically stimulated luminescence properties of the cover sands are reviewed and a

70 potential method, using thermal transfer techniques, to extend the age range of quartz OSL to
71 cover the expected age of the tektites is evaluated.

72

73

74 1.1 Sample locations

75

76 Data from investigations conducted for the tektite studies, and earlier studies where OSL
77 dates and profile measurements have been collected, have been combined to characterise the
78 general optically stimulated luminescence properties of the cover sands. The locations of
79 these samples are shown in Figure 2.

80

81 The samples from Khon Kaen (six samples between 20-200cm depths, reported by Sanderson
82 et.al., 2001), Krahad (three samples from Unit 3 between 1.1-1.8m, reported by Porat, 2017),
83 Kok Yai (three samples from Unit 3 between 0.8-1.7m reported by Porat, 2017, and two
84 further samples from the Unit 2, the meteorite impact blast granule layer, and 1m above this
85 (Unit 3) report by Cresswell et.al., 2019a) and Sa Kaeo (one sample from Unit 2 reported by
86 Cresswell et.al., 2019a) all show similar properties, with sensitive quartz ($>10^5$ cGy⁻¹) and
87 SAR-OSL ages in the 10-35ka range. Sediment profiles from these sites generally show the
88 same simple stratigraphy with depth. In contrast, samples from Huai Om (two OSL samples
89 from the base of the cover sand at a depth of 210cm and the top of the ejecta layer at a depth
90 of 295cm, plus 25 profile samples from 160-390cm depth reported in Cresswell et.al.,
91 2019a,b) and Pakse (one sample from between two possible ejecta layers reported in
92 Cresswell et.al., 2019b) contain quartz with much lower sensitivity (<5000 cGy⁻¹) and the
93 natural signals exceed the SAR-OSL saturation limit (>50 ka for these samples), the Huai Om
94 profile shows greater quartz sensitivity (comparable with the other sites) for the top sample at

95 160cm depth, with a reduction in sensitivity of more than an order of magnitude for samples
96 at 170cm depth and deeper. The basal sample from Hue (collected at 210cm depth from a
97 profile of 21 samples between 10-210cm depth reported in Cresswell et al., 2018a,b) shows a
98 mixture of both younger, sensitive quartz and older, insensitive quartz characteristic of both
99 these groups of sites. The Tad Huakhon sample (Cresswell et.al. 2019b) was collected from
100 below a currently undated lava flow and contains quartz that has high sensitivity with natural
101 OSL signals in excess of the saturation limit.

102

103 Assuming that these results from eight locations reflect regional patterns, they strongly
104 suggest that these apparently similar cover sands represent at least two different origins or
105 depositional processes. The upper layers are characterised by higher sensitivity quartz, with
106 profiles showing increasing OSL age with depth, with the samples reported here giving ages
107 in the 10-35ka range, consistent with aeolian deposition processes. The lower layers are
108 characterised by quartz with sensitivities at least two orders of magnitude lower than the
109 upper layers, and OSL dates that exceed the age range of the SAR-OSL method. The working
110 model that will be explored further in a future publication, summarised in Figure 1, is that
111 these materials are consistent with deposition by base surge following the meteorite impact
112 and subsequent air-fall processes, with later aeolian deposition of sediments from a distant
113 source.

114

115 1.2 Dating challenge

116

117 The tektites are associated with the lower layers of the cover sands which are older than the
118 SAR-OSL limit, which are virtually mono-mineralic quartz and hence luminescence dating
119 using feldspars is not an option. Thermally Transferred Optically Stimulated Luminescence

120 (TT-OSL) has been proposed as a method to access deeper traps in quartz, which are
121 expected to saturate at higher doses than the traps accessed by OSL. This approach has been
122 explored for these samples, and in this paper the approaches to use thermal transfer
123 measurements are described and the question of thermal stability at the ambient temperatures
124 of these locations addressed.

125

126 Several different protocols for TT-OSL have been used in previous studies (e.g.: Wang et.al.
127 2006a, b; Adamiec et.al. 2010; Shen et.al. 2011; Thiel et.al. 2012; Brown and Forman 2012;
128 Chapot et.al. 2016), but these all have common elements. The OSL from the sample is
129 measured as normal, then the sample is heated to an elevated temperature and kept there to
130 allow transfer of charge from deeper traps to the OSL accessible traps, and then the amount
131 of charge transferred is measured by a repeat OSL measurement (this is the TT-OSL
132 measurement). TT-OSL signals are typically 1-2% of the initial OSL. TL signals can also be
133 recorded during the ramp to the elevated temperature (TL-ramp) and during the hold phase
134 (isothermal decay – ID). Costello (2009) noted significant differences between quartz from
135 different locations through LM-OSL measurements, and noted that ID (which was described
136 as phosphorescence during the thermal transfer process) is a useful analytical approach to
137 understanding the processes. Post-OSL TL approaches, where a TL readout follows the OSL
138 measurement, also has been used previously to extend the dose response, with TL signals in
139 the 300-350°C region shown to correlate with dose (Kinnaird et.al. 2010).

140

141 Aitken (1998) proposed a model of two forms of transfer based on measurements of optical
142 bleaching at room temperature, termed ‘recuperation’ where electrons present in the OSL
143 traps are transferred to ‘refuge traps’ from where they can be transferred back to the OSL
144 traps, and ‘basic transfer’ where electrons in hard to bleach traps are transferred to the OSL

145 traps during preheating. Wang et.al. (2006a,b) demonstrated TT-OSL from fine grain (4-
146 11 μ m) quartz from Chinese loess, using 270s optical stimulation to completely remove fast
147 and medium OSL components, with heating at 260°C for 10s followed by repeat OSL
148 measurement. The resulting TT-OSL was observed to have two components attributed to
149 recuperation (ReOSL) and basic transfer (BT-OSL), with a measurement sequence proposed
150 to separate the BT-OSL and ReOSL from the total TT-OSL. Normalised ReOSL dose
151 response curves continued to grow beyond 4kGy doses with D_e values with ~20%
152 uncertainties, allowing the calculation of dates beyond 1Ma. Adamiec et.al. (2008) reported
153 experimental data supporting an alternative model for the ReOSL signals as being a single
154 transfer from traps with similar thermal stability as the fast OSL traps but only emptied
155 optically by long exposure, compared with the double transfer mechanism with refuge traps.
156 This single transfer model is then more similar to the BT-OSL process. Adamiec et.al. (2010)
157 explored the properties of these traps, again using fine (4-11 μ m) grains, proposing a protocol
158 with a 260°C 10s preheat, 200s LM-OSL at 125°C, a thermal transfer at 260°C for 10s and
159 100s CW-OSL measurement of the TT-OSL. Shen et.al. (2011) applied a modification of the
160 procedure of Wang et.al. (2006a) with transfers 300°C to different size fractions, showing no
161 significant difference in TT-OSL response as a function of grain size. Thiel et.al. (2012) used
162 a protocol proposed by Stevens et.al. (2009) (60s OSL measurements, a 260°C 10s transfer
163 and a thermally assisted optical bleaching to remove residual trapped charge (400s OSL at
164 280°C) prior to adding regenerative doses) on sand-sized (180-250 μ m) quartz grains,
165 showing that deposits older than 250ka showed an age underestimation by TT-OSL compared
166 to pIRIR measurements of K-feldspar from the same sample, attributed to thermal instability
167 in the hard to bleach traps accessed by TT-OSL. Brown and Forman (2012) adapted the
168 Stevens et.al. (2009) protocol by reducing cutheat and increasing the bleaching temperature
169 to 350°C, applied to fine grain loess. Chapot et.al. (2016) modify the procedure of Adamiec

170 et.al. (2010) using a 300s OSL rather than 80s LM-OSL, on fine grain loess.

171

172 In this paper, appropriate protocols are explored for use with the coarse grain quartz of the
173 lower sedimentary layers of the cover sands of south-east Asia, expanding on the prior work
174 summarised above. And, the thermal stability of the harder to bleach traps associated with
175 these thermally transferred signals is examined at temperatures in excess of the environments
176 of these previous studies.

177

178 2. Methods

179

180 2.1 Exploratory Analyses

181

182 As noted above, prior studies using TT-OSL have used different protocols for measurements,
183 in some instances adjusting the protocol to the samples being analysed (for example Brown
184 and Forman 2012). Some studies have also indicated variations in the parameters for the TT-
185 OSL source trap. Therefore, an exploratory analysis using two aliquots of quartz from Hue,
186 with natural signals exceeding the OSL saturation limit, was conducted with different hold
187 times (between 10 and 60s) and temperatures (between 240°C and 360°C) to determine if any
188 adjustments are needed to the protocol, and identify any significant differences in trap
189 parameters in these samples, compared to prior literature. It has already been shown that post-
190 OSL TL extends the dose range (Kinnaird et.al. 2010), in this work the use of lower
191 temperature TL is also examined. So, the luminescence signals generated during the heating
192 to transfer temperature, and hold at that temperature, are also explored as an option for
193 recovery of equivalent doses from the TT-OSL source trap.

194

195 The counts recorded during the TL-ramp, the isothermal decay (ID) during the hold and the
196 TT-OSL were used to identify the optimal protocol that maximises these signals for the
197 sample investigated. All measurements were conducted using a Risø DA-15 system, with the
198 use of low-level commands to enable measurements of photon emission during the ramp and
199 hold (TL-ramp and ID) without lowering the lift between these. The measurement steps are
200 outlined in Table 1; note that set A corresponds to the procedure of Adamiec et.al. (2010)
201 except for the use of CW OSL prior to the thermal transfer, with the “natural” dose for sets A-
202 D being any residual signal left after prior measurement cycles with these sets not including
203 the low-level commands (i.e.: the lift was lowered after the TL-ramp and raised again for the
204 hold). Figure 3 shows the TL-ramp and hold (ID) for sets E-H, where the ID measurement
205 follows immediately after the TL ramp, where it can be seen that the TL peak for these
206 samples is at about 300°C. The integrated counts for the TL-ramp and OSL measurements,
207 and the count rate for the ID, are given in Table 2. For a transfer temperature of 260°C, the
208 TT-OSL to OSL ratio is similar to that reported previously, but for higher transfer
209 temperatures the TT-OSL is very small with only the 30s hold at 280°C giving a TT-OSL
210 response. Thus, for temperatures above 280°C the OSL traps do not retain any transferred
211 charge and no TT-OSL is produced, though at these temperatures data from the transfer is
212 recorded in the TL-ramp and ID signals. A protocol with a TL-ramp to 260°C held for 30s
213 maximises the TL-ramp, ID and TT-OSL signals in the quartz from Hue used for these
214 exploratory analyses, and so will be used in subsequent analyses of the other quartz samples
215 in this study.

216

217 2.2 Application to SE Asian Cover Sand Samples

218

219 To allow direct comparison between OSL and the thermal transfer (TL-ramp, ID and TT-

220 OSL) signals, a hybrid sequence incorporating both measurements on each aliquot was used,
221 as shown in Table 3. This procedure initially records the natural OSL, TL-ramp, ID and TT-
222 OSL from the aliquots. In expectation that the thermal treatments and large doses involved in
223 the thermal transfer procedure could induce significant sensitivity changes, an OSL-SAR
224 sequence of small (1Gy) test doses and regenerative doses to 50Gy was then applied before
225 thermal transfer. After completion of the OSL-SAR sequence, a sequence of measurements of
226 the thermal transfer signals following regenerative doses from 50Gy to 1000Gy was
227 conducted. Thus, for aliquots which produce a quantified SAR-OSL equivalent dose this can
228 be directly compared with the equivalent dose produced by the three thermal transfer
229 measurements. Samples were measured in sets of 16 aliquots, divided into four sets with
230 different pre-heat temperatures used for the OSL measurements. In practice, the thermal
231 transfer signals from the 50Gy test dose were too small to allow normalisation of these
232 signals and so un-normalised TT-OSL and TL-ramp signals were used. This sequence was
233 applied to samples collected from the basal layers of the cover sands at Hue, Huai Om, Pakse,
234 Sa Kaeo and Tad Huakhon.

235

236 3. Results

237

238 A typical set of dose response curves for the three thermal transfer measurements is shown in
239 Figure 4, for a sample from Huai Om. The ID and TL-ramp signals produced during the
240 thermal transfer process are the largest signals, however they both show response curves that
241 are saturating at 600-1000Gy, and the ID natural signals are highly dispersed with many
242 exceeding the saturation value for the response curve. The TT-OSL signals are smaller, but
243 with a response curve that is only beginning to fall below linear to 1000Gy, with natural
244 signals that are tightly grouped.

245

246 The measurement sequence was applied to samples from the upper layers of cover sand,
247 which had produced well constrained OSL dates, to allow comparison between equivalent
248 dose determinations using the thermal transfer approach to the SAR-OSL equivalent doses
249 for the same aliquots. Three samples were used, two from Kok Yai and one from Sa Kaeo
250 (Cresswell et.al. 2019a), with equivalent dose values from the SAR-OSL of $4.3 \pm 0.1\text{Gy}$
251 (SUTL2990, Sa Kaeo), $10.7 \pm 0.5\text{Gy}$ and $8.6 \pm 0.1\text{Gy}$ (SUTL2987 and 2988, respectively,
252 Kok Yai). The data for each aliquot are shown in Figure 5, with linear regressions shown as a
253 guide. The precision of the data, in particular for the thermal transfer values, are low with
254 significant scatter. It is, however, clear that the slopes of regressions are significantly less
255 than one and that the thermal transfer methods significantly underestimate the E_D . It is also
256 evident that the ID data are more scattered with a large intercept and large uncertainties on
257 the regression fit. Given the poorer comparison to known age samples and greater scatter in
258 natural signals from the ID measurements, the TL-ramp and TT-OSL measurements are
259 preferred for these samples.

260

261 When applied to the samples from the basal layers of the cover sands, which are associated
262 with the tektites, the E_D values determined range from 100Gy to 250Gy (with uncertainties of
263 approximately 20% on the E_D for each sample), corresponding to ages of 70-125ka (for
264 measured dose rates mostly in the range of $1\text{-}2\text{mGy a}^{-1}$). These are significantly younger than
265 the expected ages due to the association with the tektites. It is noted that the ambient
266 temperature below 2m at the sampling locations is $26\text{-}28^\circ\text{C}$, which raises the possibility that
267 the trap accessed by the thermal transfer processes is unstable at these temperatures, hence
268 resulting in an underestimation of the age based on these measurements.

269

270 3.1 Trap Stability

271

272 The properties of the traps associated with TT-OSL have been investigated by several
273 authors. Faershtein et.al (2018) reviewed values reported by Li and Li (2006), Adamiec et.al.
274 (2010), Shen et.al. (2011), Brown and Forman (2012) and Chapot et.al. (2016) giving an
275 average E of 1.36 ± 0.45 eV and $\log_{10}s$ of $10.4 \pm 3.6 \log_{10} s^{-1}$, with calculated trap lifetimes at
276 10°C assuming first order reaction kinetics of between 10^5 and 10^9 years (average $10^{6.6 \pm 1.5}$),
277 and for Mediterranean sands they analysed E values of 1.4-1.6eV (average 1.50 ± 0.06) and
278 $\log_{10}s$ of 11.9-13.7 $\log_{10} s^{-1}$ (average 12.8 ± 0.6). Thiel et.al. (2012) measured sands from
279 Tunisia with an environmental temperature of 19°C , and observed a TT-OSL age
280 underestimation compared to pIR-IR ages from which a mean lifetime of 0.69Ma was
281 determined for the traps associated with TT-OSL, which was compared with lifetimes
282 calculated from the parameters of Adamiec et.al. 2010 which predicts a lifetime of 0.71Ma at
283 19°C . Prior literature suggests that for environmental temperatures up to 20°C the traps
284 associated with TT-OSL should have lifetimes of in the 10^5 - 10^6 a range.

285

286 The TL-ramp and ID measurements can be used to determine the properties of the TL-trap for
287 the samples analysed in this work, which follows the approach of Costello (2009). It is noted
288 that these are not high quality precision measurements of these parameters, but sufficient to
289 determine whether the properties are consistent with previously reported values. The trap
290 depth can be determined from the TL-ramp measurements, from the slope of an Arrhenius
291 plot at the rise of the TL signal. Figure 6 shows such a plot for a single aliquot, with data
292 plotted assuming the nominal temperature reported by the Risø reader is accurate (black line)
293 and for a $\pm 10\text{K}$ deviation from this (red and blue lines). Across eight aliquots used in the
294 exploratory measurements (two at each of four pre-heats) the mean value determined is 0.96

295 $\pm 0.08\text{eV}$, which after correction for thermal quenching (0.64eV) (from Wintle, 1975) gives a
296 trap depth of $1.60 \pm 0.10\text{eV}$. The fast component of the ID is then used along with this trap
297 depth to estimate the associated frequency factor for the trap, giving a result of 1.2×10^{13} to
298 $9.3 \times 10^{14} \text{ s}^{-1}$. The trap depth and frequency factors are consistent with the values previously
299 reported, as summarised above, with the frequency factor at the top end of the range of
300 previously reported values.

301

302 The lifetime for a trap can be calculated from the trap depth (E), frequency factor (s) and
303 temperature (T , in K) as $t = e^{E/kT}/s$. These values were calculated for three trap depths
304 corresponding to the range of values calculated above (1.5 , 1.6 and 1.7eV) and for the
305 corresponding frequency factors rounded to one significant figure (0.1 , 1.0 and $10 \times 10^{14} \text{ s}^{-1}$)
306 for temperatures ranging from 0 to 40°C , as shown in Table 4. It can be seen that in the 25 -
307 30°C range, typical of the ambient temperatures for deep soils in the region, the lifetimes
308 calculated for these three trap parameters are in the range of 20ka to 2Ma . For most of these
309 trap parameters at these temperatures, the calculated lifetime is short compared with the 750 -
310 800ka age of the tektites. Thus, these traps may experience thermal fading at the ambient
311 temperatures of the region, and the calculated E_D and age values for these samples may be
312 underestimated.

313

314 4. Discussion and Conclusions

315

316 Portable and laboratory luminescence profile measurements have shown a cryptostratigraphy
317 within SE Asian cover sands, with younger strata (10 - 35ka) characterised by sensitive quartz
318 and older strata characterised by low sensitivity quartz with natural signals in excess of SAR
319 saturation ($>50\text{ka}$) (Cresswell et al., 2018a, b; Cresswell et al., 2019a, b). This stratigraphy

320 suggests that there are multiple sources and processes for the development of these features,
321 with a change in sediment source and/or process no earlier than 35ka. The origins and
322 formation processes of these cover sands pose interesting questions, which would require the
323 collection of samples targeting this boundary. However, the focus of the work reported here is
324 to explore options for dating the older strata that exceed the limits of SAR-OSL.

325

326 Exploiting charge in deeper quartz traps through thermal stimulation or transfer processes
327 should allow an extension of E_D determination beyond the saturation limits of OSL
328 measurements. Previous studies have shown the potential of TT-OSL to extend ages beyond
329 1Ma. Here an exploratory analysis using a small number of aliquots has determined that a
330 ramp to 260°C and hold for 30s results in the largest TL-ramp, ID and TT-OSL signals.

331 Comparison between E_D values determined by these methods and by SAR-OSL on younger
332 samples, where there were aliquots that did not saturate, show that both TL-ramp and TT-
333 OSL methods produce an approximate linear relationship with the SAR-OSL, through data
334 with significant scatter and low precision, whereas the ID measurements on these younger
335 samples produce a highly scattered relationship with inconsistent results. Therefore, the TL-
336 ramp and TT-OSL measurements were used for measurement of the older materials.

337

338 For the samples analysed in this study, dose extension gives E_D values of 100-250Gy
339 (corresponding to ages of 70-125ka), which are significantly younger than assumed age of the
340 associated tektites within these lower layers of the cover sands. Estimates of the energy level
341 and frequency factors of these traps suggest that they are not stable over the required 0.5-
342 1.0Ma age range for dating sediments associated with tektites from an impact at 750-800ka
343 BP, at temperatures typical in SE Asia. For dating sediments of this age, which is also
344 relevant to the Brunhes-Matuyama geomagnetic reversal at a similar age, in these

345 environmental conditions a trap life time of approximately 20Ma would be needed to
346 minimize the requirement to use a significant correction for trap stability. For frequency
347 factors in the range of 10^{13} to 10^{15} s⁻¹, this would require a trap depth of at least 1.67-1.79eV.
348 Alternative methods of extending the dose range for quartz luminescence, for example photo-
349 transferred TL (PTTL), thermally assisted OSL (TA-OSL) or violet stimulated luminescence
350 (VSL) may access traps that are more thermally stable, and thus be applicable to materials
351 from locations where sediments are exposed to temperatures in excess of 20°C. These
352 alternative approaches could be considered for the materials analysed here. The dose
353 extension methods described here should be applicable to at least 500Gy (TL-ramp or ID) or
354 1kGy (TT-OSL) in more temperate locations, where temperatures rarely exceed 20°C.

355

356

357 **Acknowledgements**

358 Carling benefited from a Leverhulme Emeritus Fellowship (2016–2018) and from support in
359 the field provided by Prof. R. Tada (Japan Society for the Promotion of Science (JSPS)
360 KAKENHI Fostering Joint International Research (B) 18KK0092 (2018-2021)). The
361 luminescence analyses were part funded by the Biotechnology and Biological Sciences
362 Research Council under a Global Challenges Research Foundation Award for Global
363 Agriculture and Food Systems Research (BB/P022693/1) awarded to Darby.

364 This paper is dedicated to the memory of Paul Bishop, whose long standing interest in SE
365 Asia initiated this work.

366

367

368

369 **References**

- 370 Adamiec, G., Bailey, R.M., Wang, X.L., Roberts, H.M., Wintle, A.G., 2008. The mechanism
371 of thermally transferred optically stimulated luminescence in quartz. *J. Phys. D: Appl.*
372 *Phys.* 41 135503.
- 373 Adamiec, G., Duller, G.A.T., Roberts, H.M., Wintle, A.G., 2010. Improving the TT-OSL SAR
374 protocol through source trap characterisation. *Radiation Measurements* 45, 768-777.
- 375 Aitken, M.J., 1998. *An Introduction to Optical Dating*. Oxford University Press, Oxford
- 376 Brown, N.D., Forman, S.L., 2012. Evaluating a SAR TT-OSL protocol for dating fine-grained
377 quartz within Late Pleistocene loess deposits in the Missouri and Mississippi river
378 valleys, United States. *Quaternary Geochronology* 12, 87-97.
- 379 Chapot, M.S., Roberts, H.M., Duller, G.A.T., Lai, Z.P., 2016. Natural and laboratory TT-OSL
380 dose response curves: Testing the lifetime of the TT-OSL signal in nature. *Radiation*
381 *Measurements* 85, 41-50.
- 382 Costello, J.A.C. (2009). Physical investigations of thermally transferred optically stimulated
383 luminescence of quartz in luminescence dating. BSc Dissertation, Dept. of Physics,
384 University of Strathclyde.
- 385 Cresswell, A.J., Sanderson, D.C.W., Carling, P.A. (2018a) Luminescence Profile
386 Measurements on Samples from Vietnam Submitted by P. Carling. Technical Report.
387 SUERC, East Kilbride, UK. <http://eprints.gla.ac.uk/249340/>
- 388 Cresswell, A.J., Sanderson, D.C.W., Carling, P.A. (2018b) Dose Extension of a Sample at the
389 Base of a Sedimentary Sequence in Vietnam. Technical Report. SUERC, East
390 Kilbride, UK. <http://eprints.gla.ac.uk/249342/>
- 391 Cresswell, A.J., Sanderson, D.C.W., Carling, P.A., Darby, S. (2019a) SE Asia Agricultural
392 Soils Age Analysis. Technical Report. SUERC, East Kilbride, UK.
393 <http://eprints.gla.ac.uk/249339/>

394 Cresswell, A.J., Sanderson, D.C.W., Carling, P.A. (2019b) Luminescence Analyses of
395 Samples from Thailand and Laos. Technical Report. SUERC, East Kilbride, UK.

396 Faershtein, G., Guralnik, B., Lambert, R., Matmon, A., Porat, N. 2018. Investigating the
397 thermal stability of TT-OSL main source trap. *Radiation Measurements* 119, 102–111.

398 Jourdan, F., Nomade, S., Wingate, M. T. D., Eroglu, E., & Deino, A. (2019). Ultraprecise age
399 and formation temperature of the Australasian tektites constrained by $^{40}\text{Ar}/^{39}\text{Ar}$
400 analyses. *Meteoritics & Planetary Science*, 54, 2573–2591.

401 Kinnaird, T., Cresswell, A., Bishop, P., Sanderson, D. (2010) Luminescence Dating of
402 Samples from Raised Beaches in Tanzania. Technical Report. SUERC, East Kilbride,
403 UK. <http://eprints.gla.ac.uk/76481/>

404 Li, B., Li, S.H., 2006 .Studies of thermal stability of charges associated with thermal transfer
405 of OSL from quartz. *Journal of Physics D:Applied Physics* 39, 2941-2949.

406 Michel, V., Feng, X., Shen, G., Cauche, D., Moncel, N-H., Gallet, S., Gratuze, B., Wei, J.,
407 Ma, X., Liu, K., (2021) First $^{40}\text{Ar}/^{39}\text{Ar}$ analyses of Australasian tektites in close
408 association with bifacially worked artifacts at Nalai site in Bose Basin, South China:
409 The question of the early Chinese Acheulean. *Journal of Human Evolution* 153,
410 102953.

411 Porat, N., (2017). Thailand ages summary. Included as Appendix D to Cresswell et.al. 2019a.

412 Sanderson, D.C.W., Bishop, P., Houston, I., Boonsener, M. (2001), Luminescence
413 characterisation of quartz-rich cover sands from NE Thailand. *Quaternary Science*
414 *Reviews* 20, 893-900.

415 Shen, Z.X., Mauz, B., Lang, A., 2011. Source-trap characterization of thermally transferred
416 OSL in quartz. *J. Phys. D: Appl. Phys.* 44, 295405

417 Stevens, T., Buylaert, J.-P., Murray, A.S., 2009. Towards development of a broadly-applicable
418 SAR TT-OSL dating protocol for quartz. *Radiation Measurements* 44, 639–645.

419 Schwarz, W.H., Trieloff, M., Bollinger, K., Gantert, N., Fernandes, V.A., Meyer, H-P,
420 Povenmire, H., Jessberger, E.K., Guglielmino, M., Koeberl, C., (2016) Coeval ages of
421 Australasian, Central American and Western Canadian tektites reveal multiple impacts
422 790 ka ago. *Geochimica et Cosmochimica Acta* 178, 307–319.

423 Tada, T., Tada, R., Chansom, P., Songtham, W., Carling, P.A., Tajika, E., 2020. In situ
424 occurrence of Muong Nong-type Australasian tektite fragments from the Quaternary
425 deposits near Huai Om, northeastern Thailand. *Progress in Earth and Planetary
426 Science*, 7:66

427 Thiel, C., Buylaert, J.-P., Murray, A.S., Elmejdoub, N., Jedoui, Y., 2012. A comparison of TT-
428 OSL and post-IR IRSL dating of coastal deposits on Cap Bon peninsula, north-eastern
429 Tunisia. *Quaternary Geochronology* 10, 209-217.

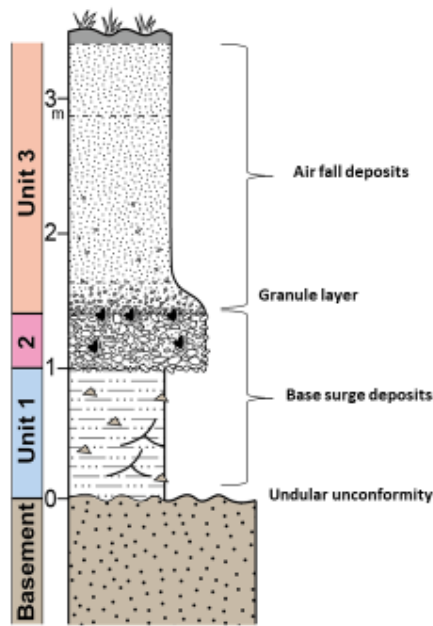
430 Wang, X.L., Lu, Y.C., Wintle, A.G., 2006a. Recuperated OSL dating of fine-grained quartz in
431 Chinese loess. *Quaternary Geochronology* 1, 89-100.

432 Wang, X.L., Wintle, A.G., Lu, Y.C., 2006b. Thermally transferred luminescence in fine-
433 grained quartz from Chinese loess: basic observations. *Radiation Measurements* 41,
434 649-658.

435 Wintle, A.G., 1975. Thermal quenching of thermoluminescence in quartz. *Geophysical
436 Journal of the Royal Astronomical Society* 41, 107-113.

437 Whymark, A., 2021. A review of evidence for a Gulf of Tonkin location for the Australasian
438 tektite source crater. *Thai Geoscience Journal* 2, 1-29.

439
440



441

442 Figure 1: Summary depositional sequence of meteorite impact deposits in south-east Asia.

443 The basement is undefined as it can vary across the region. The thicknesses of Units 1 and 2 as

444 shown are typical, although Unit 3 can be several metres thick. Unit 1 is commonly laminated

445 fine to coarse angular sand beds containing bedrock chips, local cross-bedding, and the bedding

446 grain-size varies non-systematically upwards. Unit 2 consists of unstratified to weakly

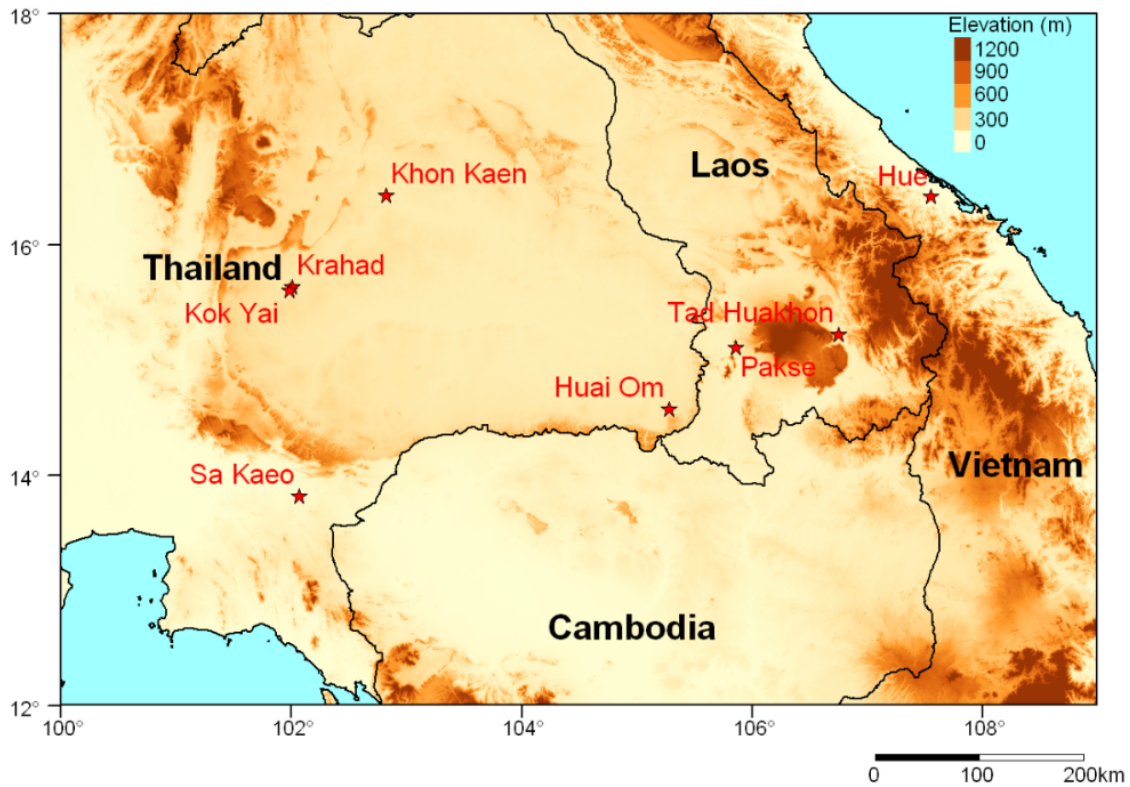
447 stratified, well-rounded white quartzite pebbles with frequent (black) tektites. Unit 3 is

448 unstratified (i.e. massive) fine to coarse sands.

449

450

451

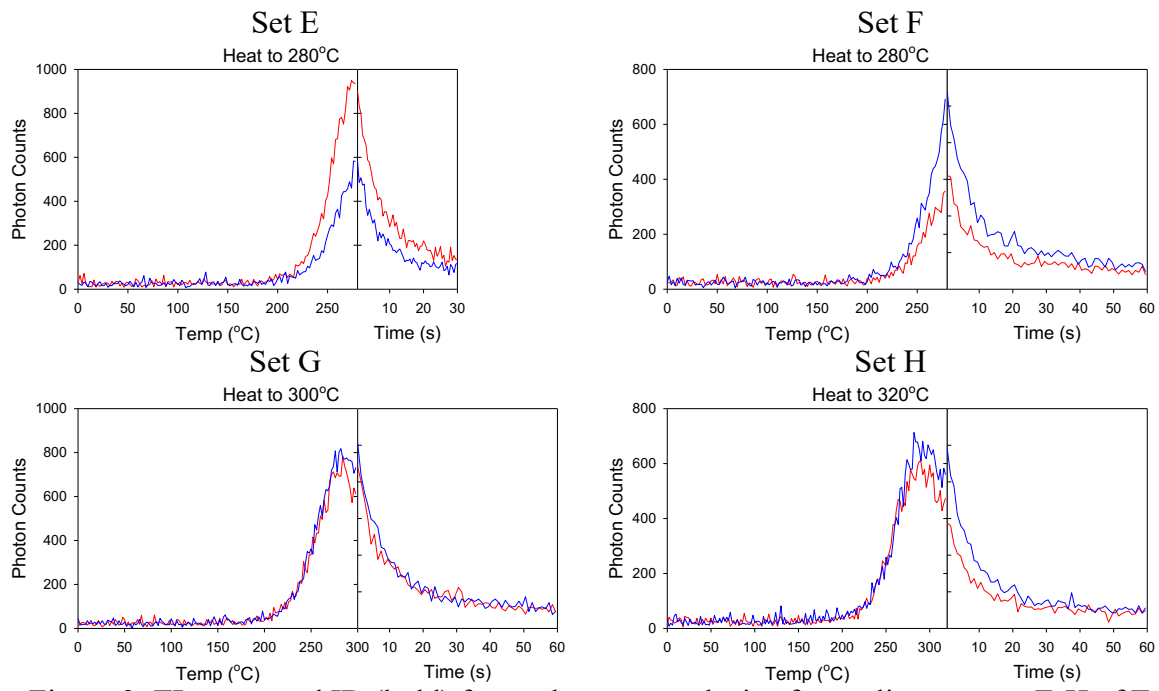


452 Figure 2: Locations of luminescence measurements of cover sands in SE Asia: Khon Kaen
 453 (Sanderson et.al. 2001); Kok Yai (Porat 2017, Cresswell et.al. 2019a); Krahad (Porat 2017);
 454 Hue (Cresswell et.al. 2018a,b); Sa Kaeo (Cresswell et.al. 2019a); Huai Om (Cresswell et.al.
 455 2019a,b); Pakse & Tad Huakhon (Cresswell et.al. 2019b).

456

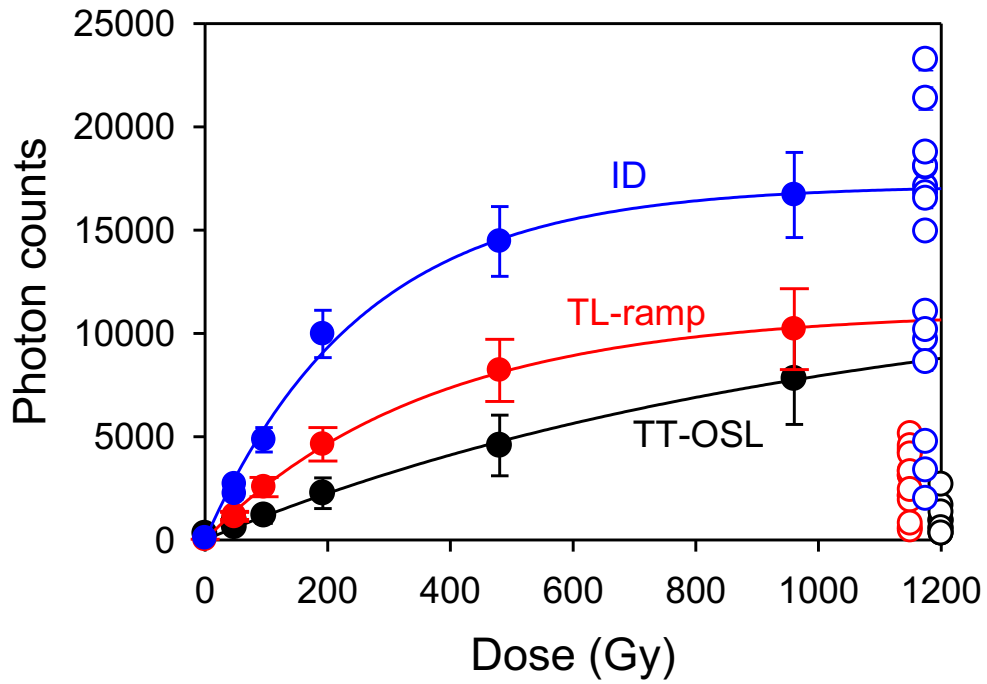
457

458



459 Figure 3: TL-ramp and ID (hold) for exploratory analysis of two aliquots, sets E-H of Table 2.

460

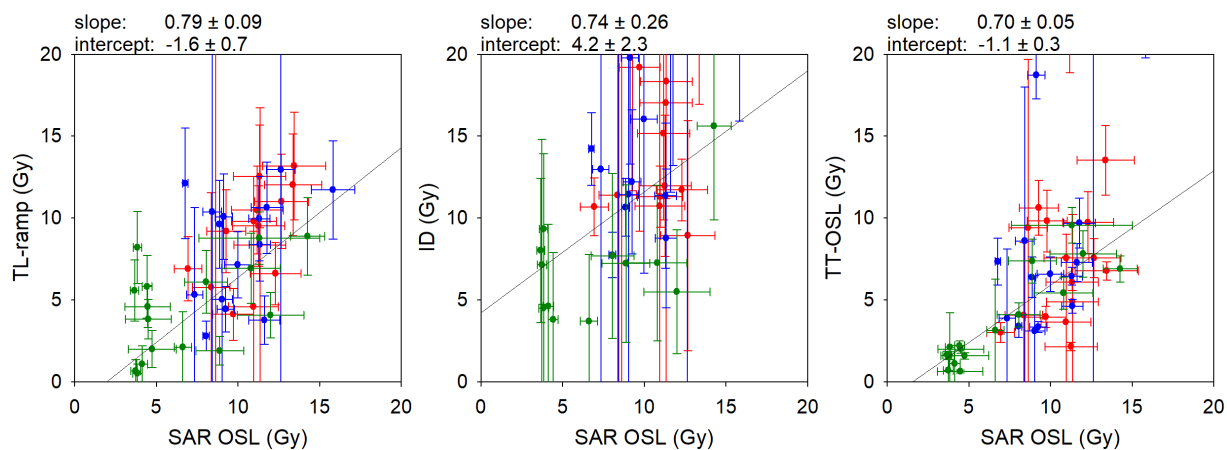


461

462 Figure 4: Dose response curves for the three thermal transfer methods, from a sample from
 463 Huai Om. The open circles on the right hand side indicate the photon counts from the natural
 464 signals for each measurement. ID measurements in blue, TL-ramp in red and TT-OSL in
 465 black.

466

467



469

470 Figure 5: Comparison between TL-ramp, ID and TT-OSL equivalent doses with the SAR-

471 OSL equivalent doses from the same aliquot, for younger samples from the upper layer of the

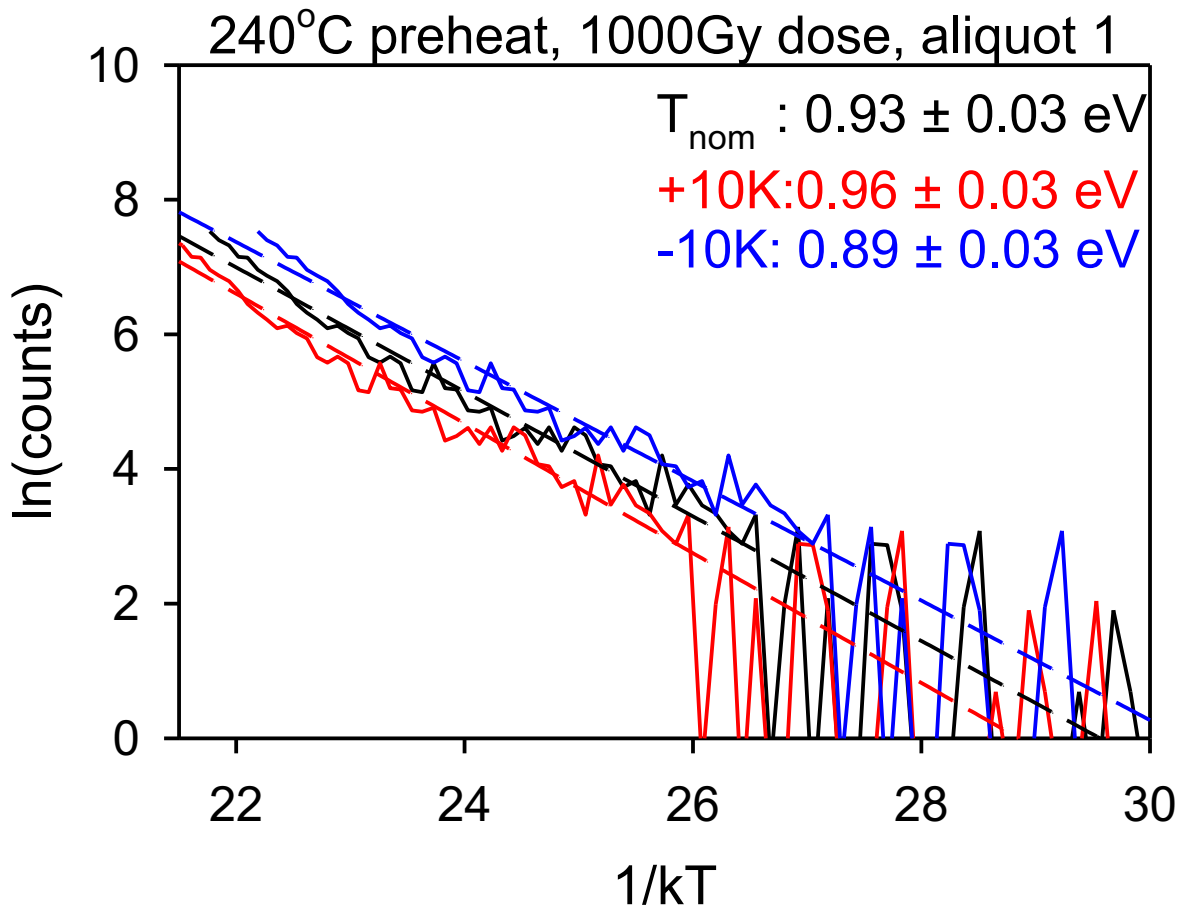
472 cover sands. Data from 16 aliquots of each of two samples from Kok Yai (blue, $E_D=8.6 \pm$ 473 0.1Gy , and red, $E_D=10.7 \pm 0.5\text{Gy}$) and a sample from Sa Kao (green, $E_D=4.3 \pm 0.1\text{Gy}$).

474

475

476

477



478 Figure 6: Example Arrhenius plot for one of 8 aliquots, showing the rising slope of the TL-
479 ramp signal and associated trap depth value, assuming the nominal temperature from the Risø
480 reader is accurate (black) and a $\pm 10\text{K}$ deviation (red and blue).

481

482

483 Table 1: Exploratory TT-OSL procedure. Set A corresponds to the procedure of Adamiec
 484 et.al. (2010).

Step	Set A	Set B	Set C	Set D	Set E	Set F	Set G	Set H
1	Dose ("natural", 100Gy, 200Gy, 500Gy, 0Gy)				Dose (200Gy)			
2	PH 260°C 10s				PH 220°C 10s			
3	OSL 100s at 125°C				OSL 100s at 125°C			
4	PH	PH	PH	PH	PH	PH	PH	PH
transfer & ID	260°C 10s	260°C 30s	280°C 10s	280°C 30s	280°C 30s	280°C 60s	300°C 60s	320°C 60s
5	OSL 100s at 125°C							
TTOSL								
6	TD (5Gy)							
7	PH 220°C 10s							
8	OSL 100s at 125°C							
9	Thermal treatment 350°C 200s							
10	Go to step 1				-			

485

486

487 Table 2: Counts for the initial OSL, TL-ramp and TT-OSL measurements for the exploratory
 488 analyses, with count rates for the ID and ratio of TT-OSL to OSL percentage.

Set	Aliquot	OSL	TL-ramp	ID cps	TT-OSL	TT-OSL : OSL %
A	1	17373 ± 146	15171	365 ± 6	354 ± 61	2.0 ± 0.4
	2	11355 ± 121	8370	228 ± 5	101 ± 58	0.9 ± 0.5
B	1	5521 ± 92	5343	139 ± 2	121 ± 52	2.2 ± 0.9
	2	35451 ± 198	8509	203 ± 3	-40 ± 60	-0.1 ± 0.2
C	1	6634 ± 102	11582	388 ± 6	250 ± 57	3.8 ± 0.9
	2	42317 ± 216	12096	464 ± 7	286 ± 60	0.7 ± 0.1
D	1	8755 ± 112	8592	275 ± 3	121 ± 57	1.4 ± 0.7
	2	23100 ± 164	8844	313 ± 3	55 ± 56	0.2 ± 0.2
E	1	22280 ± 170	18000	334 ± 9	287 ± 63	1.3 ± 0.3
	2	10760 ± 120	11007	189 ± 7	129 ± 57	1.2 ± 0.5
F	1	6120 ± 100	7888	67 ± 2	0 ± 56	0 ± 0.4
	2	30310 ± 190	10976	122 ± 2	190 ± 60	0.6 ± 0.2
G	1	20230 ± 160	20964	105 ± 2	-78 ± 54	-0.4 ± 0.3
	2	38650 ± 210	22463	115 ± 2	76 ± 60	0.2 ± 0.2
H	1	11940 ± 130	21835	65 ± 2	-10 ± 57	-0.1 ± 0.5
	2	26030 ± 180	24111	110 ± 2	141 ± 55	0.5 ± 0.2

489

490

491

492 Table 3: Outline of sequence for OSL and thermal transfer measurements on the same
 493 aliquots. Measurements were conducted in four sets (A-D) of four aliquots with different pre-
 494 heat temperatures (220°C to 280°C).

Step	Set A	Set B	Set C	Set D
1	Dose – 0Gy for natural; regen doses of 10, 20, 30, 40, 50, 0 and 10Gy for OSL SAR; regen doses of 50, 100, 200, 500, 1000, 0, & 50Gy for dose extension			
2 – PH	PH 220°C 10s	PH 240°C 10s	PH 260°C 10s	PH 280°C 10s
3 - OSL	OSL 60s at 125°C (all measurement)			
4 - TL	TL ramp to 260°C (for natural and dose extension)			
5 - ID	Isothermal decay for 30s (for natural and dose extension)			
6 - TTOSL	TT-OSL 60s at 125°C (for natural and dose extension)			
7 - TD	1 Gy Test Dose (for natural and OSL SAR)			
8 - PH	PH 220°C 10s	PH 240°C 10s	PH 260°C 10s	PH 280°C 10s
9 - OSL	OSL 60s at 125°C (for natural and OSL SAR)			
10 - TD	50 Gy Test Dose (for natural and dose extension)			
11 - PH	PH 220°C 10s	PH 240°C 10s	PH 260°C 10s	PH 280°C 10s
12 - OSL	OSL 60s at 125°C (for natural and dose extension)			
13 - TL	TL ramp to 260°C (for natural and dose extension)			
14 - ID	Isothermal decay for 30s (for natural and dose extension)			
15 -	TT-OSL 60s at 125°C (for natural and dose extension)			
TTOSL				
16	Thermal treatment 350°C 200s (for dose extension)			

495

496

497 Table 4: Lifetimes for the trap accessed by the thermal transfer processes as a function of trap
 498 depth (E), frequency factor (s) and temperature.

E (eV)	s ($\times 10^{14} \text{ s}^{-1}$)	Temperature ($^{\circ}\text{C}$)							
		0	10	15	20	25	30	35	40
1.5	0.1	13Ma	1.4Ma	470ka	170ka	62ka	24ka	9.3ka	3.8ka
1.6	1.0	100Ma	9Ma	2.9Ma	960ka	330ka	120ka	44ka	17ka
1.7	10	825Ma	64Ma	19Ma	6Ma	1.9Ma	645ka	225ka	80ka

499

500

501

502